Experiments on the sideward deflection of bedload particles

Chuanqi He[1], Ci-Jian Yang[2], and Jens Martin Turowski[3]

[1]German Research Centre for Geosciences (GFZ)
[2]German Research Centre for Geosciences
[3]GFZ German Research Centre for Geosciences, Potsdam

November 21, 2022

Abstract

Bedrock river lateral erosion plays a crucial role in landscape evolution, sediment transport and deposition, and the occurrence of geohazards. Lateral erosion is driven by the impacts of bedload particles (BPs). However, BPs generally move parallel to the channel walls and thus need to be deflected sidewards to cause wall erosion. Sideward deflection of BPs occurs when they interact with roughness elements (REs) fixed on the riverbed. We set up 21 sets of flume experiments to systematically investigate how spacing (5, 10, 20, 30, 40, 50, and 60 mm) and size (5, 10, and 20 mm) of REs influence sideward deflection of BPs. The deflection length and speed peaks at intermediate values of the spacing of REs. The likelihood for a BP to leave the roughness zone decays with the BP's distance to its edge. Our results suggest that lateral erosion rates in bedrock channels are dominantly controlled by the position of the roughness zone within the channel and its relation to the particle path.

Experiments on the sideward deflection of bedload particles

Chuanqi He[1, 2], Ci-Jian Yang[1, 3], and Jens M. Turowski[1, *]

[1] German Research Centre for Geosciences (GFZ), Potsdam 14473, Germany

[2] School of Earth Sciences, Zhejiang University, Hangzhou 310027

[3] Department of Geography, Taiwan University, Taipei 10617

***Corresponding author:**

Dr. Jens M. Turowski (turowski@gfz-potsdam.de)

Keywords: lateral erosion; flume experiment; roughness elements; bedload particles; sideward deflection

Key Points:

- For large bedload particles (10 and 20 mm), the deflection distance shows a peak at intermediate values of the spacing of roughness elements.
- The probability of leaving the roughness zone decays with the distance from its edge.
- Bedrock river lateral erosion rate is dominantly controlled by the position of roughness zone and its relation to the particle path.

Abstract:

Bedrock river lateral erosion plays a crucial role in landscape evolution, sediment transport and deposition, and the occurrence of geohazards. Lateral erosion is driven by the impacts of bedload particles (BPs). However, BPs generally move parallel to the channel walls and thus need to be deflected sidewards to cause wall erosion. Sideward deflection of BPs occurs when they interact with roughness elements (REs) fixed on the riverbed. We set up 21 sets of flume experiments to systematically investigate how spacing (5, 10, 20, 30, 40, 50, and 60 mm) and size (5, 10, and 20 mm) of REs influence sideward deflection of BPs. The deflection length and speed peaks at intermediate values of the spacing of REs. The likelihood for a BP to leave the roughness zone decays with the BP's distance to its edge. Our results suggest that lateral erosion rates in bedrock channels are dominantly controlled by the position of the roughness zone within the channel and its relation to the particle path.

1. Introduction

Fluvial bedrock erosion is a key component in landscape evolution, and thus a crucial process shaping the Earth's surface (e.g., Burbank et al., 1996; Cook et al., 2014; Scheingross et al., 2019; Turowski et al., 2013). On the landscape scale, bedrock erosion can be divided into vertical incision and lateral erosion. Vertical incision deepens the valleys, steepens the hillslopes, and is thus a primary process for landscapes to respond to the spatial-temporal variations of tectonic deformation (e.g., He et al., 2019; Larsen and Montgomery, 2012; Whittaker et al., 2007), rock resistance (e.g., Duvall et al., 2004; Sklar and Dietrich, 2001), and climate (e.g., Hartshorn et al., 2002; Murphy, et al., 2016). Compared to lateral erosion, vertical incision has received much more attention from Earth scientists (e.g., Finnegan, et al., 2014; Hartshorn et al., 2002). However, an understanding of lateral erosion is also required to model important aspects of landscape evolution, including bedrock river response to tectonic and climatic conditions, and controls on sediment transport and deposition, hillslope stability, channel width and sinuosity.

Gilbert (1877) suggested that lateral erosion happens when the channel bed is covered by alluvial deposits which inhibit vertical incision. Following the lead of Gilbert, previous research on bedrock erosion has established the role of bedload particles (BPs) supply and roughness elements (REs) on the riverbed in setting lateral erosion (e.g., Beer et al., 2017; Fuller et al., 2016; Li et al., 2020; Mishra et al., 2018; Shepherd, 1972; Turowski, 2018). Observations of the distribution of erosion across a bedrock channel in Taiwan indicate that an increase in BP supply associated with high flow events can result in coverage of riverbed, allowing channel widening (Turowski et al., 2008). Physical experiments show that an increase in BP supply can accelerate lateral erosion (e.g., Mishra et al., 2018; Shepherd, 1972). BPs generally move parallel to the channel walls. To cause lateral erosion of bedrock banks, BPs need to be sideward deflected and hit the riverbank with sufficient energy to cause erosion. Flume experiments on bedload transport over alluvial beds in a steady, uniform, and laminar flow show that, at least near the threshold of motion, BPs diffuse sidewards as they traveling downstream (Seizilles et al., 2014). Still, we know little about what controls sideward deflection length and speed. In a series of experiments, Fuller et al. (2016) demonstrated REs fixed on a riverbed show a dominant control on the sideward deflection of BPs, a notion that is supported by the field observations in a bedrock gorge in the Swiss Alps (Beer et al., 2017).

Building on these observations, we carried out 21 sets of flume experiments to systematically investigate how the spacing and size of REs affect sideward deflection of BPs and discuss the implications to bedrock river lateral erosion.

2. Methods

2.1. Experimental setup and protocol

The flume experiments were conducted at German Research Centre for Geosciences (Potsdam, Germany) in a tilting (slope = 3%) wooden flume (Figure 1). The width of the flume was 40 cm, and its total length was 190 cm, including the water tank (40×40×40 cm). BPs and REs were produced by a glass bead manufacturer in Germany (Schäfer Glas, https://www.schaeferglas.com), and had a density of 2.54 g/cm^3. Black glass spheres with a diameter of 10 mm were used as BPs, while white glass hemispheres with three diameters (5, 10, and 20 mm) were used as REs. The flume bed was painted white. REs were glued onto the riverbed in a rectangular pattern, with varying spacing and size in different experiments (Table S1; Figure S1). Water was circulated at a constant discharge of 1.6 liters/second for all of the 21 sets of experiments, yielding a flow depth of ~1.5 cm. A single BP was released from the release line across the flume, 20 cm upstream of the roughness zone (Figure 1). To ensure the impact of BPs with RE at the edge of the roughness zone, release locations were located directly upstream of the columns of REs. As a result, the number of release locations varied for different experiments (Table S1; Figure 2). From each release location, ten BPs were released, except for the release location that is above the edge of the roughness zone, where 50 BPs were released for each roughness configuration. To ensure the presence of a single particle within the flume at each time, a subsequent BP was released after the preceding BP was collected in a steel net fixed to the end of the flume. The movements of BPs were recorded continuously with a video camera located above the flume (Figure 1).

We conducted another six experiments in which several hundred BPs were released from a bucket nearly simultaneously (Movies 1 and 2). These experiments were not quantitatively analysed, but provide qualitative insights into the interaction between BPs and REs.

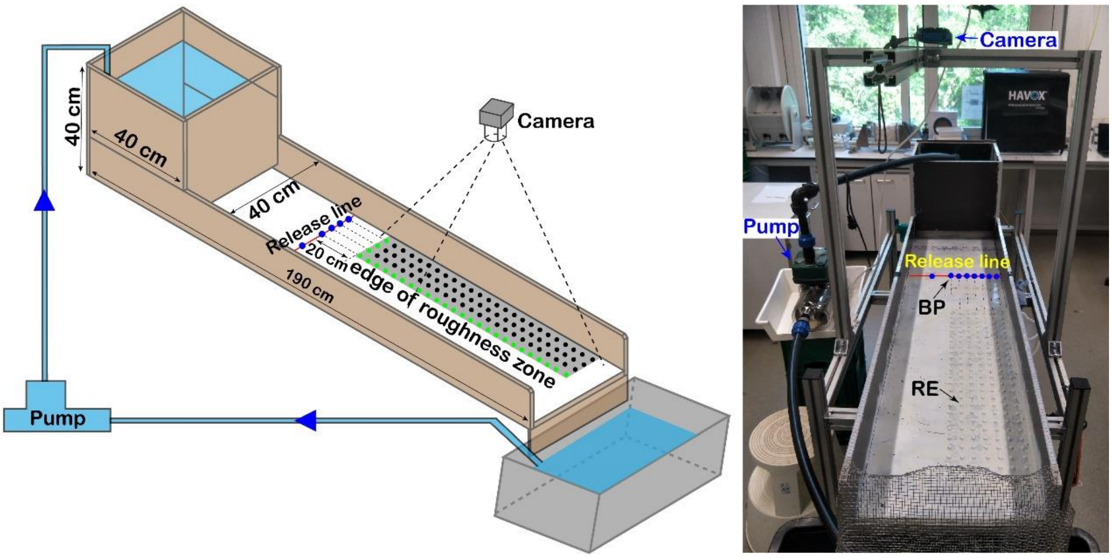

Figure 1. Experimental flume schematic and photo. The length and width of the flume was 190 cm and 40 cm, respectively, with a constant slope of 3%. The flume was made of wooden plates with a thickness of 1.6 cm. The hemispheric REs were stuck on the riverbed with water-proof glue. The length and width of the roughness zone were about 70 cm and 20 cm, respectively. The pump was a DAB ACTIV El 40/80 M, with a power of 1.48 KW. The diameter of the water-pipe was 32 mm. The camera was a Canon PowerShot D30, with a video resolution of 1920×1080 pixels. The red line marks the release line located 20 cm upstream of the roughness zone. The edge of the roughness zone was marked by green REs in the schematic illustration.

2.2. Data processing

The path of BPs was recorded on video by the camera. The captured area of the camera was the same for all the experiments. Pictures were extracted from the video every 0.1 seconds using a Python script. Pictures have a resolution of 1920×1080, and each pixel corresponds to real size of 0.564×0.564 mm at the flume bed. Using a MATLAB script (see Code

Availability), the location of BPs was marked manually on the pictures and the coordinates were extracted. From the time stamp of the picture and the time series of coordinates, we rebuilt the trajectory, and calculated velocity, deflection distance, and times of changes of the direction of motion in the cross-channel direction. We applied the two-sample Kolmogorov-Smirnov test to assess the significance of differences in the measured parameters for the different sets of experiments, i.e., the distance from the edge of the roughness zone, RE spacing, and RE size, in the control of probability of getting out of the roughness zone.

2.3. Parameters used to describe the motion of BP

To introduce the parameters effectively, we name the direction along and perpendicular to the flume the X and Y direction, respectively. In practice, it was difficult to count the impact times of each BP directly. Without impact, the Y-direction of BPs is not expected to change. Therefore, we used the number of changes in the direction of motion in the Y-direction (the Y-direction change times) as a proxy of impact times. To make different experiments with different numbers of data points within a trajectory comparable, we normalized the Y-direction change times by the total number of data points within a trajectory. For example, if a BP showed 10 Y-direction change times within 50 data points in a trajectory, the normalized Y-direction change time is 20%. The maximal Y-distance measures how far BPs can reach in Y direction from the release location. If it is larger than the Y-direction distance between the release location and the riverbank, BPs can impact the riverbank, causing lateral erosion. The total Y-direction distance is the sum of the Y-direction distance moved by BP for every two data points within a trajectory. Maximal Y-speed was defined as the largest Y-direction speed of a BP between every two data points. Average Y-speed was defined as the average Y-direction speed of a BP between every two data points. Total X- and Y-direction distance are the sum of the X- and Y-direction distance for every two data points. Total distance was calculated as the square root of the sum of the square of X-direction distance and the square of Y-direction distance. Total speed was defined as the ratio between total distance and total time.

3. Results

3.1. Trajectories of BPs

The trajectories of BPs for all experiments are displayed in Figure 2. For the smallest RE spacing of 5 mm, BPs were likely to be stopped by REs, with stopping locations moving upstream as RE size increased. Specifically, for a RE size of 5 mm, more than half of the BPs moved through the entire length of the roughness zone (Figure 2A1). For RE size of 10 mm, BPs reached the end of the flume if they laterally left the roughness zone after the first impact with a RE. BPs that remained in the roughness zone eventually be stopped (Figure 2A2). For RE size of 20 mm, 25 out of 30 BPs stopped upon the first impact with a RE, while the reminder laterally left the roughness zone after the first impact (Figure 2A3). For RE spacing greater than 5 mm, all BPs moved through the roughness zone and eventually left the flume. After the first impact with a RE, the speed of BPs decreased rapidly. BPs were deflected laterally, with an equal probability to be deflected to the left or right. As long as BPs were in the roughness zone, they repeatedly collided with REs, changing their velocities upon impact. By contrast, a fraction of BPs laterally left the roughness zone. The trajectories of BPs outside of the roughness zone follow a smooth curve, with decreasing cross-channel speed and increasing downstream speed. About half of the BPs that were released directly above the edge of the roughness zone laterally left the roughness zone after the first impact with a RE. The remaining half moved to the left into the roughness zone, but showed an average probability of 17.1% of laterally leaving the roughness zone after later impacts. The degree of concentration of trajectories is largely influenced by the spacing and size of REs. Trajectories tended to concentrate for small RE spacing and large RE size.

To qualitatively compare how the spacing and size of REs influence the trajectories of the BPs, and how BPs interact with each other, we released several hundred BPs to the flume nearly simultaneously and recorded it on video (Movies 1 and 2). In both movies, RE sizes were 5 mm (left), 10 mm (middle), and 20 mm (right). The spacing of REs was 5 mm and 10 mm in Movie 1 and Movie 2, respectively. In Movie 1, BPs travel longer downstream distances in the roughness zone with smaller RE sizes, confirm the observations from the experiments with individual BPs. In the configuration with larger RE spacing (10 mm, Movie 2), the number of BPs stopping within the roughness zone is much smaller than in the configuration with smaller RE spacing (5 mm, Movie 1). In particular, for RE size of 5 mm, nearly all BPs travel through the entire roughness zone.

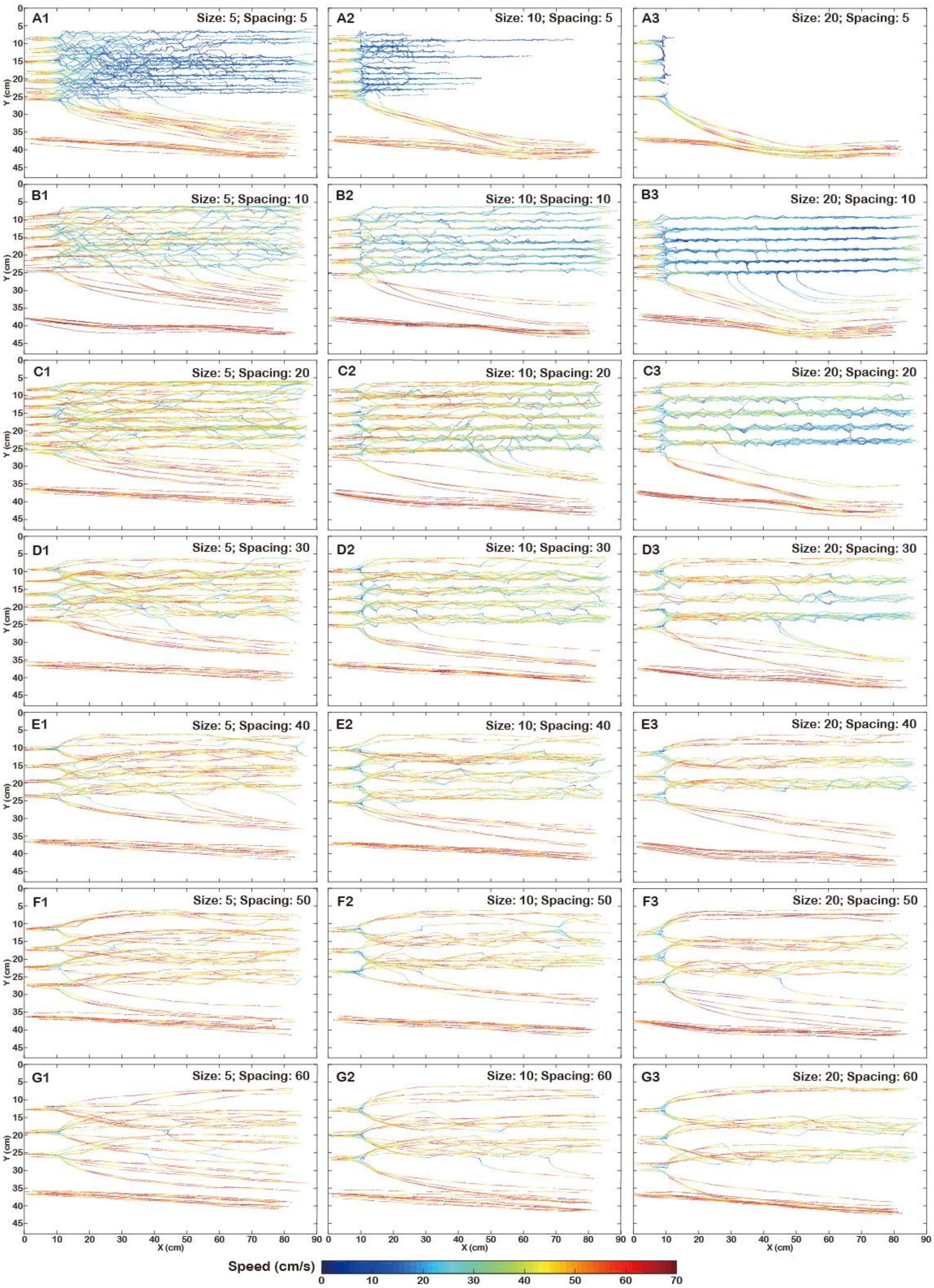

Figure 2. The trajectory and speed of BPs for the 21 sets of experiments. For each release locations shown in the figure, a single BP was released 10 times. BP locations were mapped every 0.1 seconds. Trajectory colors show the particle speed.

3.2. Sideward deflection

When BPs interacted with REs, their cross-channel direction of motion and speed changed (Figures 2 and 3). Except for two experiments (RE spacing of 5 mm, RE sizes of 10 and 20 mm) during which most BPs stopped within the roughness zone, the normalized Y-direction change times decreased with increasing RE spacing (Figure 3a). For RE sizes of 10 and 20 mm, the maximal Y-direction distances increased with increasing spacing of REs (Figure 3b). The total Y-direction distances increased with increasing RE spacing, and reached the highest values at a spacing of 20 mm before it decreased again (Figure 3c). For RE size of 5 mm, when RE spacing was small (i.e., 5 and 10 mm), BPs frequently jumped over REs leading to large maximal Y-direction distance and total Y-direction distance (Figure 3b, 3c). The maximal Y-direction distance decreased with increasing spacing until spacing reached 30 mm, then it increased with increasing spacing. Meanwhile, with the increase of RE spacing, the probability of impact decreased rapidly (Figure 3a), decreasing the total Y-direction distance (Figure 3c).

The experiments with the three different RE sizes show similar patterns in the maximal Y-speed, i.e., an increase to peak values, then decrease with increasing RE spacing (Figure 3d). Peak values were reached at a RE spacing of 10 mm for a RE size of 5 mm, at a RE spacing of 20 mm for RE size of 10 mm, and at a RE spacing of 50 mm for RE size of 20 mm. Overall, the average Y-speed shows a similar pattern as the maximal Y-speed (Figure 3e). Total speed increased with increasing RE spacing (Figure 3f).

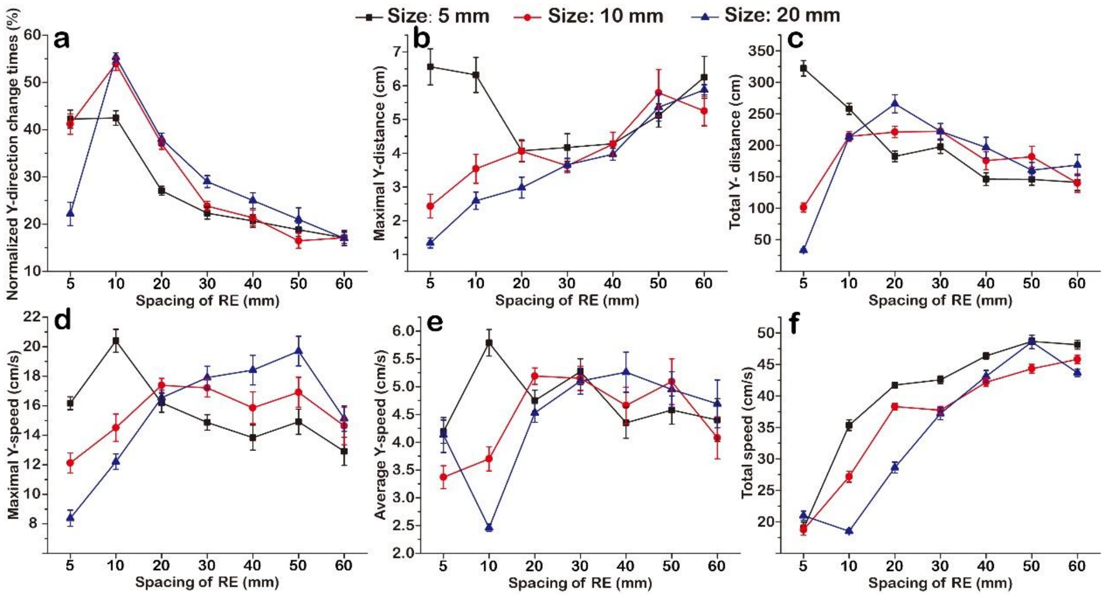

Figure 3. Statistics of particle motion as a function of spacing and size of REs.

(a) Normalized Y-direction change times, (b) maximal Y-distance, (c) total Y-distance, (d) maximal Y-speed, (e) average Y-speed, and (f) total speed varies with the spacing of REs. Errors are the standard error of the mean. See methods for the definitions of the parameters.

3.3. Escape from the roughness zone

BPs released directly above the edge of the roughness zone showed the highest probability (≥50%) of laterally escaping from the roughness zone (Figure 4). The probability decreased with the increase of Y-direction distance between the edge of the roughness zone and release location. When the distance reached 9 cm, only 1 out of 430 BPs was able to leave the roughness zone. The Kolmogorov-Smirnov test shows that these observed differences are significant at the 1% level. In contrast, experiments with different RE sizes did not yield significant differences (Figure S2).

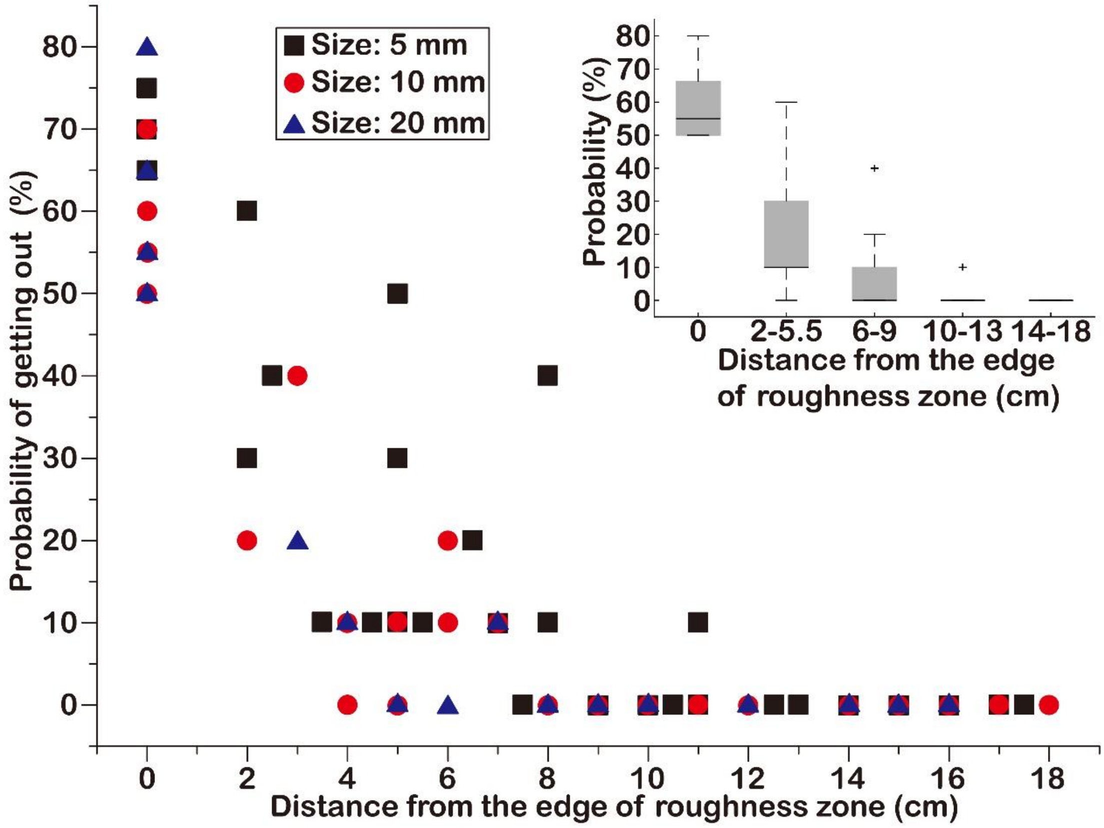

Figure 4. The probability of BPs to get out of the roughness zone. Boxplots show the probability of BPs to get out of the roughness zone in different release locations.

4. Discussion

4.1. Controls on sideward deflection of bedload particles

We observed non-monotonic relationships between the number of changes in direction (Figure 3a), the maximal and total motion in the cross-channel direction (Figure 3b, 3c), and the maximum and average cross-channel speed (Figure 3d, 3e) with RE spacing. There are several competing effects determining the lateral motion of BPs after the interaction with a RE. Relevant parameters include RE spacing, the relative size of REs and BPs, and the relative flow depth.

The observed humped function arises out of the competition between the length of the mean free path, which increases with increasing RE spacing, and the probability of a BP to impact an RE, which decreases with increasing RE spacing. As such, RE spacing has a dual role, as small spacing makes sideward motion possible in the first place, but also inhibits further lateral motion due to the limited free path. For large spacing, there is a free path for laterally movement, but low impact probability limits the chance for sideward deflection in the first place. As an example, in our experiments, for RE sizes of 10 and 20 mm, the probability of impact is high for small RE spacing (Figure 3a). However, the sideward deflection of BPs is limited by the small distance available for lateral motion. As a result, the overall sideward deflection distance is small (Figure 3b, 3c). With the increase of spacing, the total Y-direction distance increased (Figure 3c), despite the decrease of the impact probability (Figure 3a). Then, even though the spacing increased further, the total Y-direction distance decreased (Figure 3c) as does the decrease of impact probability (Figure 3a). A similar dual role of the influence of roughness on particle sideward deflection has been suggested by Turowski (2018, 2020), who argued that sideward deflection, and therefore lateral erosion, is most efficient at the edge of alluvial deposits into the direction of the bare bedrock. There, REs facilitate sideward deflection of moving particles, but because bare bedrock is smooth, sideward motion is not hindered and lateral motion distances and speeds are maximized.

In our experiments, for the smallest RE size of 5 mm and a REs spacing of 5 and 10 mm, BPs frequently jumped over REs to achieve maximal Y-direction distances (Figure 3b, 3c). The occurrence of this behavior thus seems to depend on the relative size of BPs and REs, but also on the relative flow depth, which limits the space BPs have available for motion in the vertical direction. We expect that flow velocity and channel slope also impact this behavior, with jumping becoming more frequent as flow velocity or slope increase. We have not systematically investigated these controls and further experiments will be necessary.

The existence of an optimal RE spacing and size to achieve maximal lateral erosion rate agrees with predictions by Li et al. (2020), who modelled the deflection of individual particles by REs and their effect on lateral erosion. We expect that this optimal spacing is a function of hydraulics, morphology, and sediment characteristics of a particular river. Further research is necessary to fully unravel these controls.

An interesting effect arises from the cross-channel variation of roughness, as the right-hand-half of the flume does not feature any roughness elements. This introduces secondary flow effects that strongly determine particle paths once the BPs have left the roughness zone (Figure 2; Movies 1 and 2).

4.2. Upscaling to natural rivers and implications for lateral erosion

In a natural stream, REs are unlikely to be regularly spaced, or have uniform sizes, as in the model of Li et al. (2020) and our experiments. In the case that REs within the bedrock drive sideward deflection (e.g., Beer et al., 2017), RE size and spacing are determined by the feedback between bedrock erosion, hydraulics, and sediment transport, and are likely strongly determined by lithological properties (e.g., Richardson and Carling, 2005). This feedback, the physical details of the formation of bedrock bedforms, and their lithological controls are still poorly understood (e.g., Richardson and Carling, 2005; Wilson et al., 2013). In the case that REs composed of stationary alluvial deposits drive sideward deflection, we can expect that deposited and transported sediment are drawn from the same source. Thus, both the spacing and size of RE should be of the same order as the BP size. Alluvial deposits self-organize in response to local conditions, including flow velocity, turbulence, and topography (e.g., Dreano et al., 2010; Hodge et al., 2016; Johnson and Whipple, 2010; Mishra et al., 2018). BPs would thus move over a rough surface composed out of elements similar to themselves.

In experiments of individual spherical particles moving over dry random rough surfaces composed of other spheres, driven only by gravity, four regions with different behavior have been identified. A phase diagram delineating these regions is spanned by the two axes designating the slope of the surface and the relative roughness, defined as the ratio of the size of the BP to the size of the RE (Figure 5) (e.g., Riguidel et al., 1994; Samson et al., 1998). Region A is the 'pinning' region, where the particle quickly stops independent of its initial speed. It occurs for low slopes and low relative roughness. In Region B, the particle reaches a mean downward speed after a short transient period, independent of its initial speed. In Region C, the particle showed similar behavior as in Region B, but with a mean free path that exceeded the size of the experiment. For this reason, the conditions could not be fully constrained. In Region D, the particle moves by long jumps and does not reach a steady state. In a fluvial environment, Region A corresponds to flow conditions below the threshold of motion, Regions B and C would correspond to rolling or sliding particle motion, and Region D would correspond to saltation (e.g., Drake et al., 1988). For relative roughness values of ~1, which can be expected for alluviated beds in natural rivers, the particle was in Region A for slopes of up to ~30% (Figure 5; Riguidel et al., 1994). We expect that the shear due to the flow shifts the line marking the transition from Region A to Region B to lower values of relative roughness. Given these considerations and the observations that many rivers commonly feature flow conditions close to the threshold of motion (e.g., Parker et al., 2007), and that generally only a small fraction of the available particles are moving at the same time (e.g., Wilcock and McArdell, 1993, 1997), we expect that sideward deflection is inefficient over a fully alluviated bed (cf., Seizilles et al., 2014).

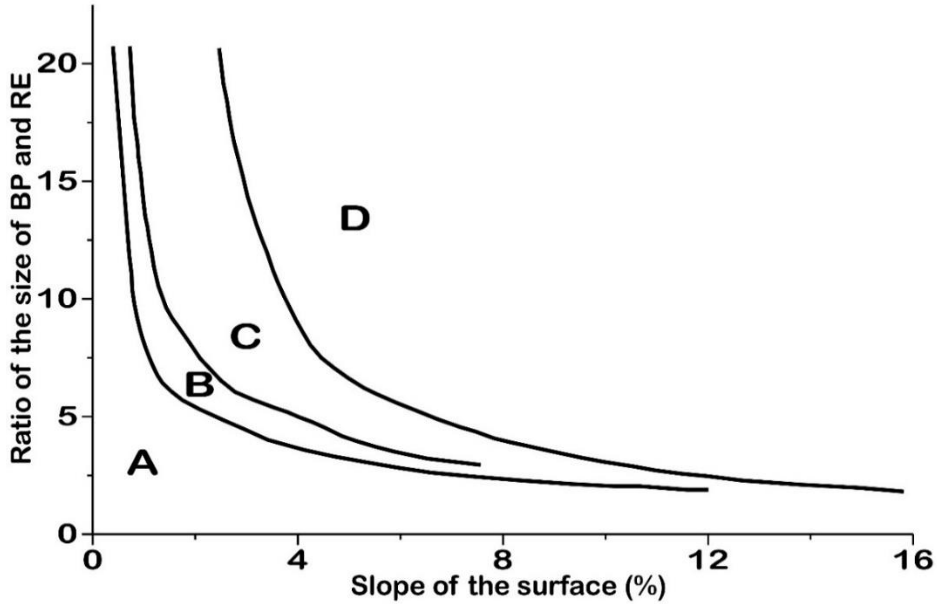

Figure 5. The relationship between the slope of the surface and the ratio of the size of BP and RE derived from experiments on gravity-driven motion on a rough slope (adopted from Riguidel et al., 1994). The figure can be divided into four regions, as marked by ‘A’, ‘B’, ‘C’, and ‘D’, respectively. In the ‘pinning’ Region A, the particle quickly comes to halt, independent of its initial velocity (no motion). In Regions B and C, after a transitory period, the particle reaches a constant steady state speed in the downslope direction (rolling or sliding motion). In region D, the particle moves by jumps longer than a single particle diameter (saltation motion).

There are two options for the deflected BPs to cause bedrock wall erosion. First, they may move on the alluvial deposit close to a bedrock wall (Figure 6a). Second, they may escape from the roughness zone to travel laterally over smooth bedrock (Figure 6a–6c) (cf., Turowski, 2018, 2020). Our experiments demonstrate that the Y-direction distance between the release location and the edge of the roughness zone plays a crucial role in determining the probability of getting out (Figure 4). In natural rivers, bedload transport is not uniform across the channel, but is concentrated along a sinusoidal path in the downstream direction (Bunte et al., 2006; Dietrich and Smith, 1984; Julien and Anthony, 2002). As a consequence, sideward deflection and lateral erosion can be expected to be effective at the locations where the bedload path interacts with stationary alluvial patches, in particular where it crosses from an alluvial patch onto the bare bedrock bed (cf. Turowski, 2018, 2020).

On the condition that BPs are unable to jump over REs and there is a bare riverbed between the riverbank and the edge of the roughness zone for BPs to move, we expect a negative correlation between lateral erosion rate and the distance between the riverbank and the edge of the roughness zone (Figure 6d). After deflected by a RE, BPs need to travel laterally to impact the riverbank. However, the cross-channel speed decreases due to the resistance of water. The larger the distance between the riverbank and the edge of the roughness zone, the less remnant cross-channel energy is available to cause lateral erosion. In addition, the increase of the distance between the edge of the roughness zone and the wall decreases the number of particles impacting the wall (Figure 6). Accordingly, we can distinguish three major cases for bedrock rivers covered by alluvial deposits. First, a riverbed is fully covered by alluvial deposits, except for a small area of bare riverbed (Figure 6a). BPs near the right riverbank can impact the wall frequently, and the majority of their kinetic energy can expended in lateral bedrock erosion. By contrast, BPs near the left riverbank can hardly impact the wall, because the REs that contact the wall can protect the wall from impacts. In this case, the two banks experience different erosion rates. Second, when the roughness zone is located at the center of the riverbed, the riverbanks are eroded at a similar rate (Figure 6b). Third, when the roughness zone is located closer to one of the riverbanks, this bank will experience a higher erosion rate, provided that the bedload concentration is symmetric across the channel. In this case, due to the erosion rate difference between the two riverbanks, the channel evolves such that the roughness zone is located at its center (Figure 6c). The erosional adjustment of channel morphology, in turn, changes flow patterns, and therefore the location of the bedload path and alluvial deposits. The formation of alluvial bedforms and the bedload path on partially covered beds are incompletely understood and need further research (e.g., Dreano et al., 2010; Jafarinik et al., 2019; Johnson and Whipple, 2010; Mishra et al., 2018).

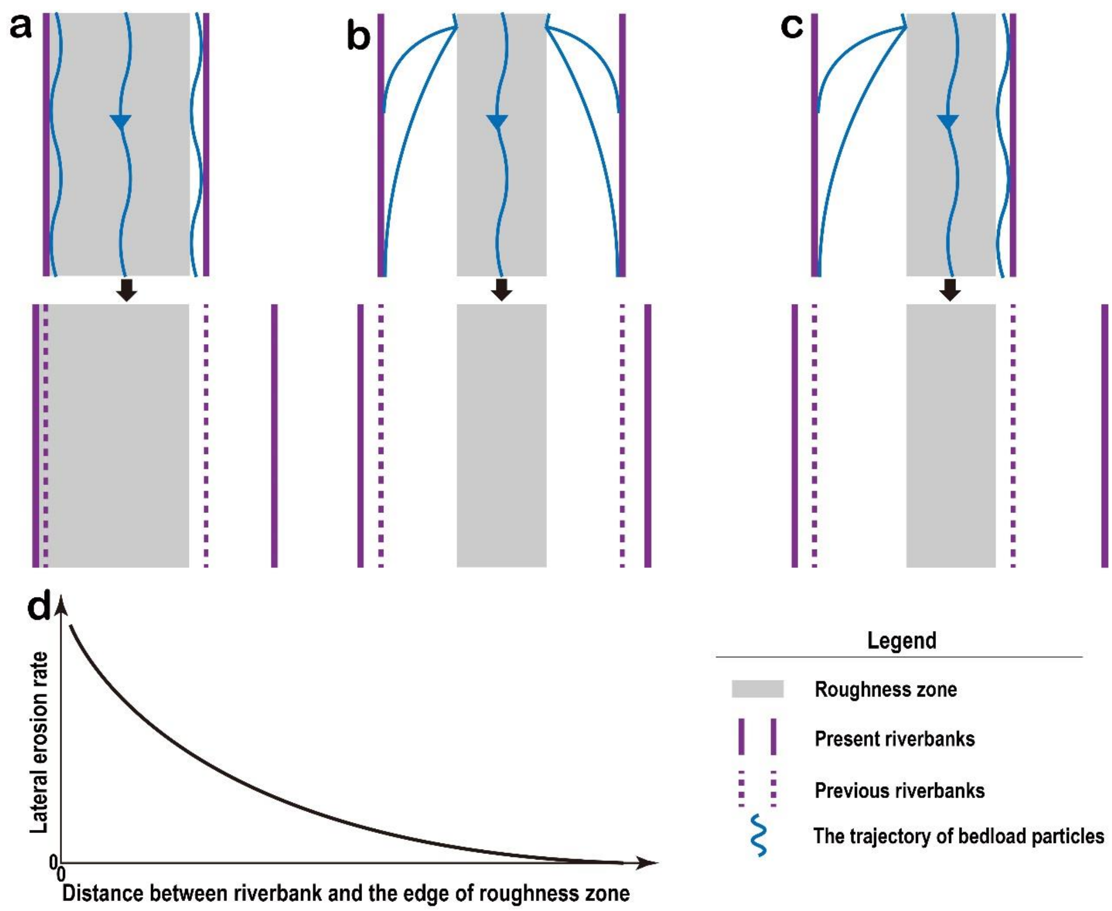

Figure 6. Illustration of how bedrock channels are laterally eroded in different settings of roughness zone under the condiction that BPs can not jump over REs. The white area within the riverbed is bare bedrock riverbed, and the grey area depicts stationary alluvial cover. (a) The riverbed is fully covered by alluvial deposits, expect a small area of bare riverbed. (b) The roughness zone is located at the center of the riverbed. (c) The roughness zone is located closer to one of the riverbanks than to the other. (d) Schematic relationship between lateral erosion rate and the distance between the riverbank and the edge of the roughness zone.

5. Conclusions

The sideward deflection distance and speed of bedload particles (BPs) were explored by 21 sets of flume experiments with different spacing and size of roughness elements (REs). The length of the free path available for BPs to move and the impact probability between BP and RE are two main factors that determine sideward deflection of BPs. Both of these two factors are necessary for BPs to achieve a high deflection length and speed. The length of the free path increases with increasing RE spacing, while the impact probability decreases with increasing RE spacing. The optimal spacing to gain the maximal sideward deflection length and speed can be expected to be a function of hydraulics, morphology, and the sediment characteristics of a particular river. Further research is necessary to unravel these controls. The size of REs affects the sideward deflection of BPs in two ways. First, in combination with RE spacing, the size of RE determines the length of the free path. Second, the relative size of BPs and REs determines whether BPs can jump over or is stopped by REs. The relative flow depth and velocity can also be expected to have an effect on this behavior, which deserve further experiments.

In natural rivers, there are two ways for deflected BPs to cause lateral erosion. First, they may move on the alluvial deposit close to a bedrock wall. Second, they may escape from the roughness zone to travel laterally over smooth bedrock. Given our observations on sideward deflection, the lateral erosion rate should show a negative relationship with the distance between the riverbank and the edge of the roughness zone. As a result, the evolution of a bedrock river and its widening rate largely depend on the location and size of roughness zones. However, the formation of alluvial deposits on bedrock beds, the evolution of roughness zones in response to hydraulics, and the bedload path need further investigation.

Acknowledgments

We are grateful to Markus Reich for flume design and help with its construction, Gunnar Pruß for purchasing roughness elements and bedload particles, as well as building the Python script to extract pictures from videos, Anne Voigtländer for help with installing the pump, and Herve Capart for providing the toolbox used by our MATLAB script (see Code Availability). Thanks go also to Brian J. Yanites and Zhenyu Peng for fruitful discussion. This work was supported by Zhejiang University Academic Award for Outstanding Doctoral Candidates to CQH and by GFZ.

Data Availability Statement

The raw data underlying Figures 2–4 were deposited in figshare with the URL: https://doi.org/10.6084/m9.figshare.12623654.v2.

Code Availability Statement

A MATLAB script (Tracking_particles.m) and its related toolbox, a readme file, and a video tutorial that can obtain the time series of coordinates from pictures were deposited in figshare with the URL: https://doi.org/10.6084/m9.figshare.12623654.v2.

References

Beer, A. R., Turowski, J. M., & Kirchner, J. W. (2017). Spatial patterns of erosion in a bedrock gorge. *Journal of Geophysical Research: Earth Surface, 122,* 191–214.

Bunte, K., Potyondy, J. P., Abt, S. R., & Swingle, K. W. (2006). Path of gravel movement in a coarse stream channel. Proceedings of the Eighth Federal Interagency Sedimentation Conference, Reno, NV, USA, 162–170.

Burbank, D. W., Leland, J., Fielding, E., Anderson, R. S., Brozovic, N., Reid, M. R., et al. (1996). Bedrock incision, rock uplift and threshold hillslopes in the northwestern Himalayas. *Nature*, *379*, 505–510.

Cook, K. L., Turowski, J. M., & Hovius, N. (2014). River gorge eradication by downstream sweep erosion. *Nature Geoscience, 7,* 682–686.

Dietrich, W. E. & Smith, J. D. (1984). Bed load transport in a river meander. *Water Resources Research, 20*, 1355–1380.

Drake, T. G., Shreve, R. L., Dietrich, W. E., Whiting, P. J., & Leopold, L. B. (1988). Bedload transport of fine gravel observed by motion-picture photography. *Journal of Fluid Mechanics, 192*, 193–217.

Dreano, J., Valance, A., Lague, D., & Cassar, C. (2010). Experimental study on transient and steady-state dynamics of bedforms in supply limited configuration. *Earth Surface Processes and Landforms, 35*, 1730–1743.

Duvall, A., Kirby, E., & Burbank, D. (2004). Tectonic and lithologic controls on bedrock channel profiles and processes in coastal California. *Journal of Geophysical Research: Earth Surface*, *109*, F03002.

Finnegan, N. J., Schumer, R., & Finnegan, S. (2014). A signature of transience in bedrock river incision rates over timescales of 10^4–10^7 years. *Nature, 505*, 391–396.

Fuller, T. K., Gran, K. B., Sklar, L. S., & Paola, C. (2016). Lateral erosion in an experimental bedrock channel: The influence of bed roughness on erosion by bed load impacts. *Journal of Geophysical Research: Earth Surface, 121*, 1084–1105.

Gilbert, G. K. (1877). Geology of the Henry Mountains (Utah). USGS Report, Government Printing Office, Washington, D.C.

Hartshorn, K., Hovius, N., Dade, W. B., & Slingerland, R. L. (2002). Climate-driven bedrock incision in an active mountain belt. *Science, 297*, 2036–2038.

He, C., Rao, G., Yang, R., Hu, J., Yao, Q., & Yang, C. J. (2019). Divide migration in response to asymmetric uplift: Insights from the Wula Shan horst, North China. *Geomorphology, 339*, 44–57.

Hodge, R., Hoey, T. B., Maniatis, G., & Lepretre, E. (2016). Formation and erosion of sediment cover in an experimental bedrock-alluvial channel. *Earth Surface Processes and Landforms, 41*, 1409–1420.

Jafarinik, S., Moreira, R. H., & Viparelli, E. (2019). Alluvial morphodynamics of bedrock reaches transporting mixed-size sand. Laboratory experiments. *Journal of Geophysical Research: Earth Surface*, *124*, 3067–3089.

Johnson, J. P., & Whipple, K. X. (2010). Evaluating the controls of shear stress, sediment supply, alluvial cover, and channel morphology on experimental bedrock incision rate. *Journal of Geophysical Research, 115*, F02018.

Julien, P. Y., & Anthony, D. J. (2002). Bed load motion and grain sorting in a meandering stream. *Journal of Hydraulic Research, 40*, 125–133.

Larsen, I. J., & Montgomery, D. R. (2012). Landslide erosion coupled to tectonics and river incision. *Nature Geoscience, 5*, 468–473.

Li, T., Fuller, T. K., Sklar, L. S., Gran, K. B., & Venditti, J. G. (2020). A Mechanistic Model for Lateral Erosion of Bedrock Channel Banks by Bedload Particle Impacts. *Journal of Geophysical Research: Earth Surface, 125*, e2019JF005509.

Mishra, J., Inoue, T., Shimizu, Y., Sumner, T., & Nelson, J. M. (2018). Consequences of Abrading Bed Load on Vertical and Lateral Bedrock Erosion in a Curved Experimental Channel. *Journal of Geophysical Research: Earth Surface*, *123*, 3147–3161.

Murphy, B. P., Johnson, J. P., Gasparini, N. M., & Sklar, L. S. (2016). Chemical weathering as a mechanism for the climatic control of bedrock river incision. *Nature*, *532*, 223–236.

Parker, G., Wilcock, P. R., Paola, C., Dietrich, W. E., & Pitlick, J. (2007). Physical basis for quasi-universal relations describing bankfull hydraulic geometry of single-thread gravel bed rivers. *Journal of Geophysical Research*, *112*, F04005.

Richardson, K., & Carling, P. A. (2005). A typology of sculpted forms in open bedrock channels. Geol. Soc. Am., Boulder, Colorado, 108 pp.

Riguidel, F., Jullien, R., Ristow, G., Hansen, A., & Bideau, D. (1994). Behaviour of a sphere on a rough inclined plane. *Journal de Physique I, 4*, 261–272.

Samson, L., Ippolito, I., Batrouni, G. G., & Lemaitre, J. (1998). Diffusive properties of motion on a bumpy plane. *The European Physical Journal B*, *3*, 377–385.

Scheingross, J., Lamb, M. P., & Fuller, B. M. (2019). Self-formed bedrock waterfalls. *Nature*, *567*, 229–233.

Seizilles, G., Lajeunesse, E., Devauchelle, O., & Bak, M. (2014). Cross-stream diffusion in bedload transport. *Physics of Fluids, 26*, 013302.

Shepherd, R. G. (1972). Incised river meanders: Evolution in simulated bedrock. *Science, 178*, 409–411.

Sklar, L. S., & Dietrich, W. E. (2001). Sediment and rock strength controls on river incision into bedrock. *Geology, 29*, 1087–1090.

Turowski, J. M., Hovius, N., Hsieh M.-L., Lague, D., & Chiang, M.-C. (2008). Distribution of erosion across bedrock channels. *Earth Surface Processes and Landforms, 33*, 353–363.

Turowski, J. M., Badoux, A., Leuzinger, J., & Hegglin, R. (2013). Large floods, alluvial overprint, and bedrock erosion. *Earth Surface Processes and Landforms, 38*, 947–958.

Turowski, J. M. (2018). Alluvial cover controlling the width, slope and sinuosity of bedrock channels. *Earth Surface Dynamics, 6*, 29–48.

Turowski, J. M. (2020). Mass balance, grade, and adjustment timescales in bedrock channels. *Earth Surface Dynamics, 8*, 103–122.

Whittaker, A. C., Cowie, P. A., Attal, M., Tucker, G. E., & Roberts, G. P. (2007). Bedrock channel adjustment to tectonic forcing: Implications for predicting river incision rate. *Geology, 35*, 103–106.

Wilcock, P. R., & McArdell, B. W. (1993). Surface-based fractional transport rates: Mobilization thresholds and partial transport of a sand-gravel sediment. *Water Resources Research, 29*, 1297–1312.

Wilcock, P. R., and McArdell, B. W. (1997). Partial transport of a sand/gravel sediment. *Water Resources Research, 33*, 235–245.

Wilson, A., Hovius, N., & Turowski, J. M. (2013). Upstream-facing convex surfaces: Bedrock bedforms produced by fluvial bedload abrasion. *Geomorphology, 180–181*, 187–204.